



Brazilian Journal of Physics

ISSN: 0103-9733

luizno.bjp@gmail.com

Sociedade Brasileira de Física

Brasil

Singh Gautam, Manjeet

Role of Projectile Degrees of Freedom in Sub-Barrier Fusion Dynamics

Brazilian Journal of Physics, vol. 46, núm. 2, abril, 2016, pp. 143-151

Sociedade Brasileira de Física

São Paulo, Brasil

Available in: <http://www.redalyc.org/articulo.oa?id=46444888002>

- How to cite
- Complete issue
- More information about this article
- Journal's homepage in redalyc.org

redalyc.org

Scientific Information System

Network of Scientific Journals from Latin America, the Caribbean, Spain and Portugal

Non-profit academic project, developed under the open access initiative

# Role of Projectile Degrees of Freedom in Sub-Barrier Fusion Dynamics

Manjeet Singh Gautam<sup>1</sup>

Received: 16 November 2015 / Published online: 4 January 2016  
© Sociedade Brasileira de Física 2016

**Abstract** This work theoretically investigates the role of the projectile degrees of freedom on the fusion dynamics of various heavy-ion fusion reactions. The impact of the projectile breakup channel is studied for the fusion mechanism of the  ${}^8_4\text{Be} + {}^{89}_{39}\text{Y}$ ,  ${}^{12}_6\text{C} + {}^{89}_{39}\text{Y}$ , and  ${}^{32,34}_{16}\text{S} + {}^{89}_{39}\text{Y}$  reactions within the view of the coupled channel approach and the energy-dependent Woods-Saxon potential model (EDWSP model). The above-barrier fusion cross-section data of the  ${}^8_4\text{Be} + {}^{89}_{39}\text{Y}$  reaction is suppressed by about 20 % with respect to the theoretical predictions of the coupled channel approach and the single barrier penetration model while this suppression factor is reduced to 10 % within the context of the EDWSP model calculations. Such fusion hindrance at above-barrier energies can be understood in terms of the projectile breakup effects that arise due to its low breakup threshold. However, the observed fusion enhancement of the  ${}^{12}_6\text{C} + {}^{89}_{39}\text{Y}$  and  ${}^{32,34}_{16}\text{S} + {}^{89}_{39}\text{Y}$  reactions, wherein the colliding pairs are stable against breakup, is adequately explained by the EDWSP model and the coupled channel approach in the whole range of energy around the Coulomb barrier. This reveals that the energy dependence in the nucleus-nucleus potential governs barrier modification effects (barrier height, barrier position, barrier curvature) in closely similar way as reflected from the coupled channel formulation.

**Keywords** Heavy-ion near-barrier fusion reactions · Coupled channel equations · Weakly bound nuclei

**PACS No.** 25.60.Pj · 21.60.Ev · 24.10.Eq

## 1 Introduction

Heavy-ion fusion reactions at energies lying in the close vicinity of the Coulomb barrier are strongly influenced by the internal structure of the colliding pairs. In the past few years, the role of nuclear structure degrees of freedom of the interacting nuclei, like static deformation, inelastic surface excitations, and nucleon transfer channels, on the fusion process has been extensively analyzed for many projectile-target combinations. In the case of tightly bound nuclei, it has been well accepted that the coupling to nuclear structure degrees of freedom of the fusing systems results in a substantially large sub-barrier fusion enhancement in comparison to the expectations of the single barrier penetration model [1]. The coupling of the intrinsic channel of the collision partners to their relative motion leads to a distribution of barriers of different height and weight and consequently produces an anomalously large fusion enhancement at sub-barrier energies. However, the situation gets more complex in fusion reactions involving weakly bound systems due to their breakup effects. As a result of low breakup threshold, the weakly bound nuclei may break before reaching the fusion barrier and consequently reduce the entrance channel flux going into the fusion channel. This kind of physical effect leads to the suppression of the fusion excitation function data at above-barrier energies. The magnitude of the suppression factor depends upon the breakup threshold of the weakly bound system. The recent advancement in the field of radioactive beam facilities in different laboratories around the world has triggered the interest in understanding the role of the breakup channel in the fusion process. The availability of precise measurements of fusion cross sections for weakly bound stable nuclei like  ${}^6_3\text{Li}$  and  ${}^9_4\text{Be}$  increases the

✉ Manjeet Singh Gautam  
gautammanjeet@gmail.com

<sup>1</sup> School of Physics and Material Science, Thapar University, Patiala, Punjab 147004, India

possibilities of exploring the fusion dynamics of loosely bound systems [2].

The breakup thresholds of these nuclei vary from 1.475 MeV to 2.45 MeV and hence they have significant breakup probabilities. In the last few decades, the influence of the breakup channel of weakly bound nuclei on the fusion process has been extensively studied and the literature shows that the complete fusion cross-section data at above-barrier energies is substantially hindered with respect to the coupled channel calculations and the single barrier model calculations [3–11]. However, a priori estimates of fusion enhancement or fusion suppression induced by the loosely bound system cannot be made due to the fact that their breakup channel involves the coupling to continuum states. Dasgupta et al. [12] have shown that the above barrier fusion excitation function data of the  ${}^6_3\text{Li} + {}^{209}_{83}\text{Bi}$  and  ${}^9_4\text{Be} + {}^{208}_{82}\text{Bi}$  reactions is suppressed by  $\sim 30\%$  with respect to the coupled channel calculations. In the case of the  ${}^9_4\text{Be} + {}^{144}_{62}\text{Sm}$  reaction, the fusion suppression of  $10\%$  at above-barrier energies has been pointed out [13–15]. Rath et al. [16–18] observed a fusion suppression of  $32\%$  for the  ${}^6_3\text{Li} + {}^{144}_{62}\text{Sm}$  reaction, and  $26\%$  for the  ${}^6_3\text{Li} + {}^{152}_{62}\text{Sm}$  and  ${}^7_3\text{Li} + {}^{144}_{62}\text{Sm}$  reactions. Hagino et al. [19] have shown that the involvement of the breakup channel results in a larger fusion cross section at sub-barrier energies, while it leads to inhibition of the above-barrier fusion data. Diaz-Torres et al. [20] based on continuum discretized coupled channel (CDCC) calculations arrived at similar conclusions. However, the different theoretical approaches lead to controversial conclusions with regard to the fusion enhancement/fusion suppression due to the breakup channel. Therefore, in order to contribute to the investigation of the role of the breakup channel on the fusion process, the fusion dynamics of the  ${}^9_4\text{Be} + {}^{89}_{39}\text{Y}$  reaction has been theoretically analyzed in the present work. The reason for choosing this reaction is of manifold like low breakup threshold of the projectile, light target isotope, and the breakup of the projectile may occur via different channels with the different breakup probabilities. Furthermore, the fusion dynamics of the  ${}^9_4\text{Be} + {}^{89}_{39}\text{Y}$  reaction is compared with the fusion mechanism of the stable projectiles with a common target isotope ( ${}^{89}_{39}\text{Y}$ ). The comparison of the fusion excitation functions of the  ${}^9_4\text{Be} + {}^{89}_{39}\text{Y}$ ,  ${}^{12}_6\text{C} + {}^{89}_{39}\text{Y}$ , and  ${}^{32,34}_{16}\text{S} + {}^{89}_{39}\text{Y}$  reactions reveals that the above barrier fusion excitation function data of the  ${}^9_4\text{Be} + {}^{89}_{39}\text{Y}$  reaction is suppressed with reference to that of the  ${}^{12}_6\text{C} + {}^{89}_{39}\text{Y}$  and  ${}^{32,34}_{16}\text{S} + {}^{89}_{39}\text{Y}$  reactions [21, 22]. The theoretical calculations of the fusion excitation functions are obtained using the energy-dependent Woods-Saxon potential model (EDWSP model) [23–30] and the coupled channel approach [31]. The single barrier penetration model calculations and the

coupled channel calculations predict larger fusion cross sections for the  ${}^9_4\text{Be} + {}^{89}_{39}\text{Y}$  reaction by an amount of  $20\%$  at above barrier energies. In contrast to this, the EDWSP model-based calculations reduce the magnitude of the suppression factor by an amount of  $10\%$ , and hence, the above barrier fusion excitation function data of the  ${}^9_4\text{Be} + {}^{89}_{39}\text{Y}$  reaction is hindered by an order of  $10\%$  with respect to the expectations of the EDWSP model calculations. A brief description of the theoretical formalism adopted in this article is presented in Sect. 2. The results of the theoretical calculations are discussed in detail in Sect. 3, and the summary of the work is presented in Sect. 4.

## 2 Theoretical Formalism

### 2.1 Single Channel Description

The partial wave fusion cross section is defined as

$$\sigma_F = \frac{\pi}{k^2} \sum_{\ell=0}^{\infty} (2\ell + 1) T_{\ell}^F \quad (1)$$

The tunneling probability ( $T_{\ell}^F$ ) based on the parabolic approximation of the effective interaction potential between heavy ions was proposed by Hill and Wheeler and is given by the following expression [32]:

$$T_{\ell}^{HW} = \frac{1}{1 + \exp\left[\frac{2\pi}{\hbar\omega_{\ell}} (V_{\ell} - E)\right]} \quad (2)$$

This parabolic approximations were further simplified by Wong using the following assumptions for barrier position, barrier curvature, and barrier height [33].

$$\begin{aligned} R_{\ell} &= R_{\ell=0} = R_B \\ \omega_{\ell} &= \omega_{\ell=0} = \omega \\ V_{\ell} &= V_B + \frac{\hbar^2}{2\mu R_B^2} \left[ \ell + \frac{1}{2} \right]^2 \end{aligned}$$

where  $V_B$  is the Coulomb barrier which corresponds to  $\ell=0$ .

Using the above assumptions and by taking the effects of the infinite number partial waves, one obtains the following expression for the one-dimensional Wong formula for the evaluation of fusion excitation functions [33].

$$\sigma_F = \frac{\hbar\omega_B^2}{2E} \ell n \left[ 1 + \exp\left(\frac{2\pi}{\hbar\omega} (E - V_B)\right) \right] \quad (3)$$

In the recent work, the EDWSP model [23–30] has been exploited to explain the observed fusion dynamics of tightly bound systems wherein it has shown that the energy

dependence in nucleus-nucleus potential introduces similar kinds of the barrier modification effects as evident from the usual coupled channel approach. This work has been extended to explore the fusion dynamics of the projectile-target combinations involving weakly bound system. In the EDWSP model, the standard Woods-Saxon potential is modified by introducing the energy dependence in the diffuseness parameter. The choice of the standard Woods-Saxon potential is defined as

$$V_N(r) = \frac{-V_0}{\left[1 + \exp\left(\frac{r-R_0}{a}\right)\right]} \quad (4)$$

where  $R_0 = r_0\left(A_P^{\frac{1}{3}} + A_T^{\frac{1}{3}}\right)$ . The quantity “ $V_0$ ” is strength, and “ $a$ ” is diffuseness parameter of the Woods-Saxon potential. In the EDWSP model, the depth of real part of the Woods-Saxon potential is defined by the following expression:

$$V_0 = \left[A_P^{\frac{2}{3}} + A_T^{\frac{2}{3}} - (A_P + A_T)^{\frac{2}{3}}\right] \left[2.38 + 6.8(1 + I_P + I_T) \frac{A_P^{\frac{1}{3}} A_T^{\frac{1}{3}}}{(A_P^{\frac{1}{3}} + A_T^{\frac{1}{3}})}\right] \text{ MeV} \quad (5)$$

where  $I_P = \left(\frac{N_P - Z_P}{A_P}\right)$  and  $I_T = \left(\frac{N_T - Z_T}{A_T}\right)$  are the isospin asymmetry of the colliding systems. In fusion dynamics, the various kinds of static and dynamical physical effects such as variations of  $N/Z$  ratio, variations of surface energy and surface diffuseness of the colliding pairs, variations of nucleon densities in the neck region, and dissipation of kinetic energy of the relative motion to internal structure degrees of freedom of the fusing nuclei occur in the surface region of the nuclear potential. These physical effects produce the modification in the values of parameters of the standard Woods-Saxon potential and consequently bring the requirement of the larger diffuseness parameter for accounting the observed fusion data [1, 2, 34–36]. In addition, the surface region of the nuclear potential ( $r \geq R_P + R_T$ ) is more sensitive to small change in the nucleon density parameters than the inner region, and the nuclear structure effects of the colliding nuclei are dominant at the surface region and are mainly related to the diffuseness parameter of the nuclear potential. The authors of the ref. [37] showed that the strengths of the nuclear potential in the region near the barrier position may vary about 25 % due to nuclear structure effects and this variation of the nuclear potential in surface region is associated with modifications of the diffuseness parameter. Furthermore, the energy dependence in the nuclear potential arises due to non-local quantum effects as well as due to the presence of channel coupling effects [37–39]. In order to extract unambiguous picture of the nuclear reaction dynamics, such physical effects must be incorporated in the theoretical models. Therefore, owing to the importance of the diffuseness parameter, the energy dependence in

the Woods-Saxon potential is taken via its diffuseness parameter which takes care of the all above mentioned physical effects in sub-barrier fusion dynamics. In the EDWSP model calculations, the energy-dependent diffuseness parameter is defined as

$$a(E) = 0.85 \left[ 1 + \frac{r_0}{13.75 \left(A_P^{\frac{1}{3}} + A_T^{\frac{1}{3}}\right) \left(1 + \exp\left(\frac{\frac{E}{V_{B0}} - 0.96}{0.03}\right)\right)} \right] \text{ fm} \quad (6)$$

In the EDWSP model calculations, this expression provides a wide range of the diffuseness parameter depending upon the value of  $r_0$  and bombarding energy of the relative motion. In the present model, the value of the range parameter ( $r_0$ ) is adjusted in order to vary the diffuseness parameter in order to vary the diffuseness parameter required to address the observed fusion excitation function data of the colliding system under consideration. As all three potential parameters, ( $r_0$ ,  $a$ , and  $V_0$ ) are interrelated with each other and the variation in one parameter automatically brings the corresponding change in the values of other parameters. In the present model, the value of  $V_0$  depends upon the surface energy and isospin term of colliding pairs while the other two parameters ( $r_0$  and  $a$ ) are related through the Eq. (6). Therefore, the variation of diffuseness parameter is controlled by the range parameter ( $r_0$ ). In the EDWSP model, the range parameter ( $r_0$ ) geometrically defines the radii  $\{R_0 = r_0(A_P^{\frac{1}{3}} + A_T^{\frac{1}{3}})\}$  of the colliding systems as done in usual coupled channel calculations [1, 2, 31, 40, 41]. Therefore, the value of the range parameter strongly depends on the nuclear structure as well as on the nature of dominance of nuclear structure degrees of freedom of the fusing pairs like inelastic surface excitations, static deformation, and nucleon (multi-nucleon) transfer channels. The values of range parameter used in the EDWSP model calculations are consistent with the commonly adopted values of the range parameter ( $r_0 = 0.90 \text{ fm}$  to  $r_0 = 1.35 \text{ fm}$ ) used in literature within the context of the different theoretical methods for different fusing systems [1, 2, 35–42]. In the present analysis, the values of the range parameter extracted for the  ${}^9_4\text{Be} + {}^{89}_{39}\text{Y}$ ,  ${}^{89}_{6}\text{C} + {}^{89}_{39}\text{Y}$ , and  ${}^{32,34}_{16}\text{S} + {}^{89}_{39}\text{Y}$  reactions are also consistent with our previous analysis [23–30, 43–47].

## 2.2 Coupled Channel Description

This section deals with a brief review of the coupled channel formulation wherein the internal structure degrees of freedom of the colliding pairs can be explicitly included. From theoretical point of view, the role of nuclear structure degrees of freedom like inelastic surface excitations, static deformation,

nucleon transfer channels, etc. can be adequately addressed within the framework of the coupled channel formulation. In the coupled channel calculations, it is quite difficult to include the impacts of all the intrinsic degrees of freedom but one can entertain the influences of dominant channels [31, 40, 41]. In this method, the following set of the coupled channel equation is solved numerically.

$$\left[ \frac{-\hbar^2}{2\mu} \frac{d^2}{dr^2} + \frac{J(J+1)\hbar^2}{2\mu r^2} + V_N(r) + \frac{Z_P Z_T e^2}{r} + \varepsilon_n - E_{cm} \right] \psi_n(r) + \sum_m V_{nm}(r) \psi_m(r) = 0 \quad (7)$$

where  $\vec{r}$  is the radial coordinate for the relative motion between the fusing systems.  $\mu$  is defined as the reduced mass of the fusing pairs.  $E_{cm}$  and  $\varepsilon_n$  are bombarding energy in the center of mass frame and the excitation energy of the  $n^{th}$  channel, respectively.  $V_{nm}$  is the matrix elements of the coupling Hamiltonian, which in the collective model consists of the Coulomb and nuclear components. The coupled channel calculations are performed by using the code CCFULL [31] wherein the coupled channel equations are solved numerically by using no-Coriolis or rotating frame approximation and ingoing wave boundary conditions (IWBCs). The rotating frame approximation has been used to reduce the dimension of the coupled channel equations [31, 40, 41]. In the condition of no transfer of the angular momentum from the relative motion of the reactants to their intrinsic motion, the total orbital angular momentum quantum number  $L$  can be replaced by the total angular momentum quantum number  $J$ . This approximation is also known as the isocentrifugal approximation. Under this approximation, the number of coupled channel equation reduced to great extent. For instance, in this approximation, the  $z$ -axis is taken in the direction of the relative separation  $\vec{r}$  of the colliding systems so that  $\theta=0$  and the spherical harmonics become  $Y_{\lambda\mu}^*(\hat{r}) = \sqrt{\frac{2\lambda+1}{4\pi}} \delta_{\mu,0}$ . This implies that the excited states of each nucleus will have same spin projection on the rotating  $z$ -axis as in the respective ground states and the numbers of the coupled channel equations to be solved are significantly reduced. For example, the multi-pole excitation  $0^+ \rightarrow \lambda$  is represented by only one channel in this approximation whereas  $(\lambda+1)$  channels are required in the full problem. Specifically, if one wants to entertain  $0^+$ ,  $2^+$ ,  $4^+$ , and  $6^+$  rotational states of the deformed nucleus, a set of 16 coupled channel equations is to be solved, but in rotating frame approximation, one has to solve only four coupled channel equations. The IWBCs, which are well applicable for the heavy-ion reactions, are used to obtain the numerical solution of the coupled channel equations. According to IWBC, there are only incoming waves at the minimum position of the Coulomb pocket inside the barrier and there are

only outgoing waves at the infinity for all channels except for the entrance channel. The code CCFULL exploited the static Woods-Saxon potential for the theoretical predictions of the fusion excitation functions. Therefore, by incorporating the appropriate number of the relevant channels, the fusion cross section becomes

$$\sigma_F(E) = \sum_J \sigma_J(E) = \frac{\pi}{k_0^2} \sum_J (2J+1) P_J(E) \quad (8)$$

where  $P_J(E)$  is the total transmission coefficient corresponding to the angular momentum  $J$ .

### 3 Results and Discussion

The optimum choice of the nucleus-nucleus potential is a crucial input for the theoretical models used to analyze the nuclear reaction studies, and in heavy-ion fusion dynamics, the different forms of the nuclear potential have been extensively used to explain the observed behavior of the fusion excitation function data [1, 2, 37–39]. In this regard, the present work uses the static Woods-Saxon potential and the EDWSP model to explain the fusion dynamics of the  ${}^9_4\text{Be} + {}^{89}_{39}\text{Y}$ ,  ${}^{12}_6\text{C} + {}^{89}_{39}\text{Y}$ , and  ${}^{16}_8\text{O} + {}^{89}_{39}\text{Y}$  reactions. The values of the deformation parameters and the corresponding excitation energies of low lying  $2^+$  and  $3^-$  vibrational states of the fusing nuclei are listed in Table 1. The barrier height, barrier position, and barrier curvature of the colliding systems used in the EDWSP model calculations along with the one-dimensional Wong formula are listed in Table 2. The potential parameters like range, depth, and diffuseness parameters used in the EDWSP model calculations for the chosen reactions are listed in Table 3.

The collision partners being spherical in shape exhibit collective surface vibrational states as the dominant mode of couplings. In the earlier work, the fusion dynamics of the tightly bound projectile-target systems has been adequately explored using the EDWSP model. In the recent work, the fusion mechanism of  ${}^6_3\text{Li} + {}^{208}_{82}\text{Pb}$  reaction has been analyzed wherein the suppression factor of 34 % with respect to the EDWSP model calculations was pointed out at above barrier energies [43]. Here, this work has been extended to explore the role of the projectile breakup channel for the heavier projectile ( ${}^9_4\text{Be}$ ) on fusion process. For this purpose, the fusion

**Table 1** The deformation parameter ( $\beta_\lambda$ ) and the energy ( $E_\lambda$ ) of the quadrupole and octupole vibrational states of the colliding nuclei

Nucleus	$\beta_2$	$E_2$ (MeV)	$\beta_3$	$E_3$ (MeV)	Reference
${}^{12}_6\text{C}$	0.592	4.440	0.440	9.640	[48, 49]
${}^{32}_{16}\text{S}$	0.320	2.230	0.400	5.006	[22]
${}^{34}_{16}\text{S}$	0.240	2.130	0.390	4.620	[22]
${}^{89}_{39}\text{Y}$	0.104	2.011	0.208	2.742	[22]



**Table 2** The values of  $V_{B0}$ ,  $R_B$ , and  $\hbar\omega$  used in the EDWSP model calculations for the chosen reactions

System	$V_{B0}$ (MeV)	$R_B$ (fm)	$\hbar\omega$ (MeV)	Reference
${}^9_4\text{Be} + {}^{89}_{39}\text{Y}$	21.60	9.63	3.76	[21]
${}^{12}_6\text{C} + {}^{89}_{39}\text{Y}$	31.83	9.88	4.10	[21]
${}^{32}_{16}\text{S} + {}^{89}_{39}\text{Y}$	78.28	10.52	3.60	[22]
${}^{34}_{16}\text{S} + {}^{89}_{39}\text{Y}$	77.48	10.64	3.49	[22]

dynamics of the different projectiles ( ${}^9_4\text{Be}$ ,  ${}^{12}_6\text{C}$ , and  ${}^{32,34}_{16}\text{S}$ ) are studied with a common target isotope ( ${}^{89}_{39}\text{Y}$ ) so that an unambiguous conclusion about the impacts of the projectile breakup channel can be extracted. The coupled channel analysis of the chosen reactions will be discussed in Figs. 2 and 3. In Fig. 1, the roles of the barrier modification effects that occur due to the energy dependence in the nucleus-nucleus potential are presented. Due to the energy dependence in the nucleus-nucleus potential, the energy-dependent Woods-Saxon potential becomes more attractive in the vicinity of the Coulomb barrier and consequently modifies the barrier characteristics of the interaction barrier between the colliding systems. This results in a spectrum of the energy-dependent fusion barriers of different height. In the spectrum of the energy-dependent fusion barriers, the height of some fusion barriers is smaller than that the Coulomb barrier which, in turn, allows the maximum penetration of the entrance channel flux to fusion channel. The splitting of the single fusion barrier into a spectrum of the energy-dependent fusion barrier represents similar physically behavior as inferred from a barrier distribution produced in the coupled channel calculations. As a consequence of the energy dependence in the nucleus-nucleus potential, the EDWSP model effectively lowers the fusion barrier between the colliding systems just in a similar way as reflected from the coupled channel calculations and hence predicts significantly larger fusion excitation functions in reference to the calculations based on the static Woods-Saxon potential. The barrier modification effects are basic physical mechanism of the

**Table 3** Range, depth, and diffuseness of the Woods-Saxon potential used in the EDWSP model calculations for chosen reaction

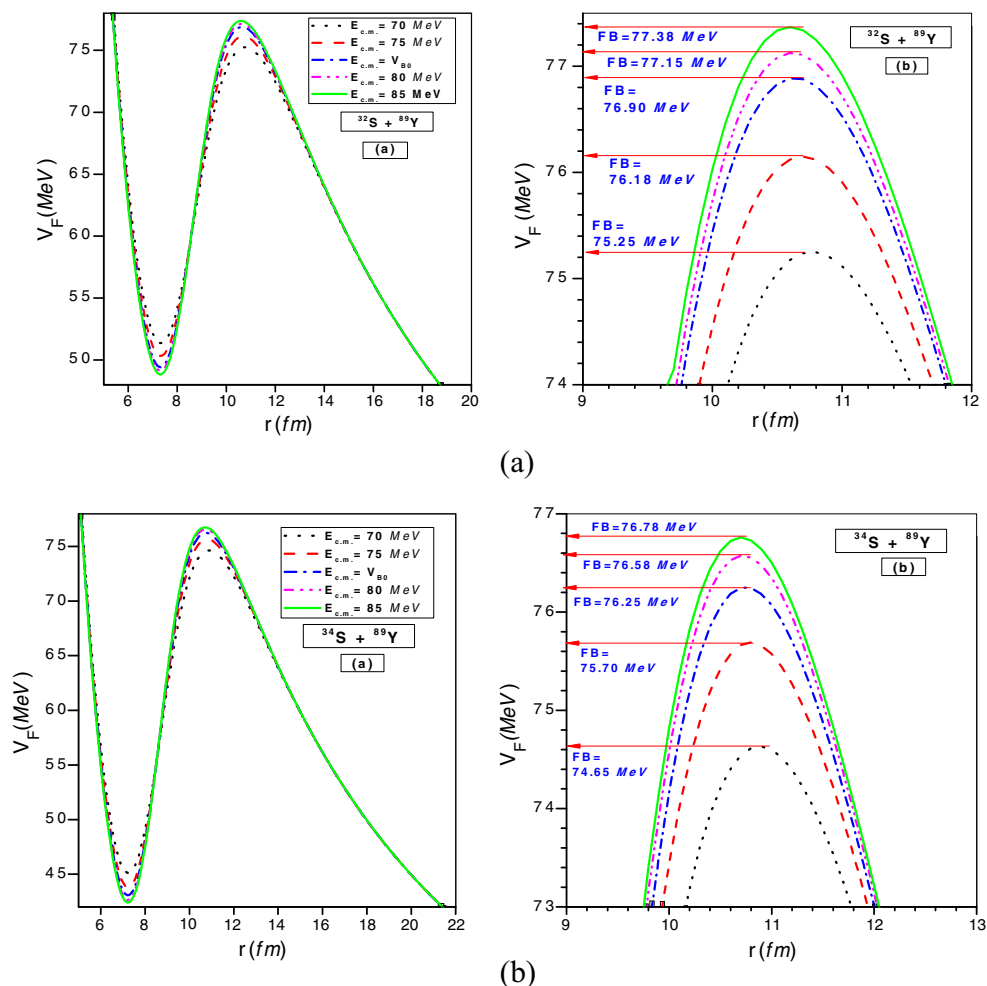
System	$r_0$ (fm)	$V_0$ (MeV)	$\frac{a^{\text{Present}}}{\text{Energy Range}} \left( \frac{\text{fm}}{\text{MeV}} \right)$
${}^9_4\text{Be} + {}^{89}_{39}\text{Y}$	1.060	42.94	$\frac{0.94 \text{ to } 0.85}{15 \text{ to } 35}$
${}^{12}_6\text{C} + {}^{89}_{39}\text{Y}$	1.090	48.62	$\frac{0.95 \text{ to } 0.85}{25 \text{ to } 45}$
${}^{32}_{16}\text{S} + {}^{89}_{39}\text{Y}$	1.116	91.88	$\frac{0.97 \text{ to } 0.85}{70 \text{ to } 95}$
${}^{34}_{16}\text{S} + {}^{89}_{39}\text{Y}$	1.107	99.71	$\frac{0.96 \text{ to } 0.85}{70 \text{ to } 95}$

EDWSP model, and barrier lowering effects consistently result in an adequate explanation of the observed fusion dynamics of various heavy-ion fusion reactions. In Fig. 1, the details of barrier modification effects for the  ${}^{32,34}_{16}\text{S} + {}^{89}_{39}\text{Y}$  reactions, wherein the possibilities of the breakup channel can be completely ruled out and the concrete conclusions about the role of the breakup channel on fusion process are directly evident, are presented.

In EDWSP model calculations, at below barrier energies, the value of the diffuseness parameter is largest ( $a=0.97\text{ fm}$  for the  ${}^{32}_{16}\text{S} + {}^{89}_{39}\text{Y}$  reaction and  $a=0.96\text{ fm}$  for the  ${}^{34}_{16}\text{S} + {}^{89}_{39}\text{Y}$  reaction) which, in turn, results in the lowest fusion barrier. For the  ${}^{32}_{16}\text{S} + {}^{89}_{39}\text{Y}$  system, the lowest fusion barrier produced at largest diffuseness parameter ( $a=0.97\text{ fm}$  and  $E_{c.m.}=70\text{ MeV}$ ) is  $75.25\text{ MeV}$  (for the  ${}^{34}_{16}\text{S} + {}^{89}_{39}\text{Y}$  reaction,  $FB=74.65\text{ MeV}$ ). The difference between the lowest fusion barrier produced in the EDWSP model and Coulomb barrier is  $3.03\text{ MeV}$  for the  ${}^{32}_{16}\text{S} + {}^{89}_{39}\text{Y}$  system and  $2.83\text{ MeV}$  for the  ${}^{34}_{16}\text{S} + {}^{89}_{39}\text{Y}$  system. The presence of such fusion barrier physically accounts for the shifting of maximum flux from the entrance channel to fusion channel. As bombarding energy increases, the diffuseness parameter reduces from  $a=0.97\text{ fm}$  to  $a=0.85\text{ fm}$  which, in turn, increase the height of the corresponding fusion barrier from  $75.25\text{ MeV}$  to  $77.38\text{ MeV}$  for the  ${}^{32}_{16}\text{S} + {}^{89}_{39}\text{Y}$  system ( $74.65\text{ MeV}$  to  $76.78\text{ MeV}$  for the  ${}^{34}_{16}\text{S} + {}^{89}_{39}\text{Y}$  system). At above barrier energies, the fusion cross section is almost independent of the nuclear structure effects and consequently gets saturated at above barrier energies. This physical effect is adequately incorporated in the present model calculations wherein the diffuseness parameter gets saturated at above barrier energies to its minimum value ( $a=0.85\text{ fm}$ ). At such energies, the fluctuation in the height of the fusion barrier becomes negligibly small and physically represents the insensitivity of the fusion excitation function toward nuclear structure effects. At well above the barrier ( $E_{c.m.}=85\text{ MeV}$ ,  $a=0.85\text{ fm}$ ), the largest fusion barrier for the  ${}^{89}_{39}\text{S} + {}^{89}_{39}\text{Y}$  system is  $77.38\text{ MeV}$  (for the  ${}^{34}_{16}\text{S} + {}^{89}_{39}\text{Y}$  reaction,  $FB=76.78\text{ MeV}$ ) which is smaller than that of the Coulomb barrier as listed in Table 2. The barrier lowering effects, which are the main stem of the EDWSP model, lead to an adequate explanation of the sub-barrier fusion enhancement of the various heavy-ion fusion reactions. The similar kinds of the barrier modification effects are found for the  ${}^9_4\text{Be} + {}^{89}_{39}\text{Y}$  and  ${}^{12}_6\text{C} + {}^{89}_{39}\text{Y}$  reactions.

In ref. [38, 39, 50, 51] based on time-dependent microscopic Hartree-Fock theory, authors have explicitly shown that the coupling between the relative motion and internal structure degrees of freedom of the colliding pairs strongly affect the fusion barrier by dynamically modifying the densities of the colliding nuclei. Due to variation of the nucleon densities of the colliding systems, the single Coulomb barrier splits into a group of the energy-dependent fusion barriers. The different fusion barrier at different bombarding energy automatically includes all the dynamical effects and hence completely explained the observed fusion

**Fig. 1** The fusion barrier (FB) for the  $^{32,34}\text{S} + ^{89}\text{Y}$  reactions obtained using the EDWSP model [23–30]



dynamics of various heavy-ion fusion reactions. In similar fashion, the EDWSP model results in a spectrum of the energy-dependent fusion barriers and approximately regulates the influence of the nuclear structure degrees of freedom as well as the dynamical effects which arises due to the fluctuations of the nucleon densities of the interacting nuclei.

The details of the coupled channel calculations for the  $^8\text{Be} + ^{89}\text{Y}$  reaction are shown in Fig. 2. The projectile ( $^8\text{Be}$ ) is the most suitable candidate to examine the role of the breakup channel on fusion reactions. This projectile has large breakup probability due to its low binding energy. The breakup of the projectile may proceed either via  $^8\text{Be} + n$  channel or  $^4\text{He} + ^4\text{He} + n$  channel with a breakup threshold of 1.57 MeV or  $^4\text{He} + ^4\text{He}$  channel with a breakup threshold of 2.47 MeV.  $^5\text{He}$  is an unbound system which finally leads to  $^4\text{He} + n$ . Therefore, the projectile ( $^8\text{Be}$ ) has a large probability of the breaking up into two alpha particles which, in turn, hinders the complete fusion yields. The breakup of the projectile is a result of the excitation of the  $^8\text{Be}$  nucleus to energies above the threshold value for one or more decay channel and consequently dissociates into alpha particles. This excitation energy may be mediated either via Coulomb field or nuclear

field of the target isotope. The breakup of the projectile via Coulomb field occurs with the population of resonant states (sequential breakup) and extended to energies far below

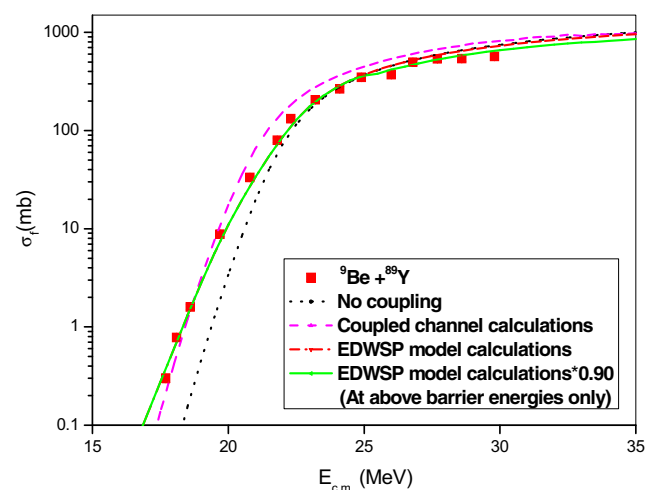


**Fig. 2** The fusion excitation functions of the  $^8\text{Be} + ^{89}\text{Y}$  reaction obtained using the EDWSP model and the coupled channel code CCFULL. The results are compared with the available experimental data taken from ref. [21]

classical fusion barrier. The nuclear breakup is a non-resonant (direct breakup) that arises from the continuum states. The  ${}^9_4\text{Be}$  nucleus has no bound excited state but has the resonance states in the continuum at  $E^* = 2.43\text{ MeV}$  corresponding to the  $\frac{5}{2}^-$  state and  $E^* = 6.81\text{ MeV}$  corresponding to the  $\frac{7}{2}^-$  state of the  $K = \frac{3}{2}^-$  ground state rotational band. The chosen reactions lying in the medium mass region  $A = 80$  to  $A = 100$  are primarily investigated with the aim to check out whether the suppression of the fusion cross section occurs in medium mass region or not. The target isotope is a neutron magic nucleus, and therefore, the influences of the coupling to low lying inelastic surface excitations are expected to be less than that for the heavier target isotope ( ${}^{144-154}_{62}\text{Sm}$ ,  ${}^{197}_{79}\text{Au}$ ,  ${}^{208}_{82}\text{Pb}$ ,  ${}^{209}_{83}\text{Pb}$ , and  ${}^{238}_{92}\text{U}$ ). In addition to this, the chosen target isotope is monoisotopic and the contribution to some evaporation residues (ERs) formed from the other isotopes can be ruled out. This unambiguously single out the role of the breakup channel on fusion process. The effects of the breakup channel on fusion excitation functions are incorporated through the coupled channel calculations performed using a modified version of code CCFULL [31] wherein the couplings to projectile excited states have been properly included. The couplings to one phonon  $2^+$  vibrational state alone or  $3^-$  vibrational states alone of the target cannot address the observed sub-barrier fusion data of the  ${}^9_4\text{Be} + {}^{89}_{39}\text{Y}$  reaction. The effects of the  $3^-$  vibrational state of the target isotope are found to be more pronounced as compared to the other inelastic surface excitations, and therefore, the inclusion of the one phonon  $2^+$  vibrational and two phonon  $3^-$  vibrational states improves the theoretical predictions but still unable to account the observed fusion excitation function data. This suggests that the projectile excitations must be included in the coupled channel description in order to explain the sub-barrier fusion data. The addition of  $\frac{5}{2}^-$  and  $\frac{7}{2}^-$  state of the  $K = \frac{3}{2}^-$  ground state rotational band of the projectile along with two phonon vibrational states in the target isotope reasonably address below barrier fusion data, but this over predicts to the experimental fusion data in above barrier energy regions by an amount of 20 %. On the other hand, this fusion hindrance is minimized within the view of the EDWSP model-based calculations by an order of 10 %, and hence, the above barrier fusion data of the  ${}^9_4\text{Be} + {}^{89}_{39}\text{Y}$  reaction is hindered by a factor of 10 % with reference to the EDWSP model predictions as shown in Fig. 2. This fusion inhibition is a consequence of the projectile breakup effects that occur due to its low binding energy.

In order to track the isotopic dependence of the sub-barrier fusion enhancement, the fusion dynamics of the different projectiles ( ${}^{12}_6\text{C}$  and  ${}^{32,34}_{16}\text{S}$ ) are examined with a common target isotope ( ${}^{89}_{39}\text{Y}$ ) wherein inelastic surface excitation is dominant. The different theoretical results along with the experimental fusion data of the chosen reactions are shown in Fig. 3. In the case of the  ${}^{12}_6\text{C} + {}^{89}_{39}\text{Y}$  reaction, the experimental data is strongly under-predicted by the theoretical results based on no coupling assumption. The couplings to one phonon  $2^+$  and  $3^-$

vibrational states in the projectile alone or one phonon  $2^+$  and  $3^-$  vibrational states in the target alone are unable to recover the experimental data particularly at below barrier energies, but the above barrier fusion data is adequately addressed by such couplings. To overcome the large deviations between above coupling scheme and the below barrier fusion data, the addition of higher multi-phonon vibrational states of the target isotope is essentially required. The inclusions of two phonon vibrational states in the target as well as the single phonon vibrational states in the projectile result in an accurate description of the observed fusion dynamics of the  ${}^{12}_6\text{C} + {}^{89}_{39}\text{Y}$  reaction as shown in the Fig. 3a. In the case of the EDWSP model calculations, as a consequence of the barrier lowering effects (see Fig. 1), the theoretical results provide complete description of the fusion excitation function data of the chosen reaction in the whole range of energy as depicted in Fig. 3a. This clearly mirrors the fact that the energy dependence in the nucleus-nucleus potential mimics the dominant influence of the inelastic surface excitations of the fusing systems.

With a common projectile, the larger sub-barrier fusion enhancement is expected for the neutron-rich target isotope and henceforth can be correlated with the increase of collective nature as well as the large probability of the neutron transfer channels with positive ground state  $Q$  values. In the case of the fusing systems, wherein a series of the target isotopes of a given element is involved but ruled out the possibilities of the neutron transfer channels instead of giving strong isotopic dependence of the sub-barrier fusion enhancement will display a mild isotopic effects on fusion process. The fusion of the  ${}^{32,34}_{16}\text{S} + {}^{89}_{39}\text{Y}$  systems [22] is an example of such interest wherein the coupling to proton (nucleon) transfer channel seems to be undesirable. The different behavior of the fusion excitation functions of the  ${}^{16}_{89}\text{S} + {}^{89}_{39}\text{Y}$  systems in the sub-barrier energy regions clearly reflects the difference in the nuclear structure of the projectiles. In the case of the  ${}^{32,34}_{16}\text{S} + {}^{89}_{39}\text{Y}$  systems, the probability of the proton transfer channels with positive ground state  $Q$  values is quite large which, in turn, expected to produce substantially larger sub-barrier fusion cross section. It is well recognized that the coupling to the neutron transfer channel with positive  $Q$  value produces a noticeable fusion enhancement at sub-barrier energies [1, 2] but the puzzling behavior of the proton transfer couplings on the fusion dynamics has not been fully recovered because only few candidates are available for such investigation. Unlike for neutron transfer, the proton transfer leads to change in the Coulomb energy which must be taken into consideration as protons are the charge particles. The fusion of the  ${}^{32,34}_{16}\text{S} + {}^{89}_{39}\text{Y}$  systems has been considered to elucidate the effects of proton transfer channel on fusion mechanism. The projectiles, which are differing in their structure, possess inelastic surface vibrations only. Furthermore, the fusion of the  ${}^{32}_{16}\text{S} + {}^{89}_{39}\text{Y}$  system



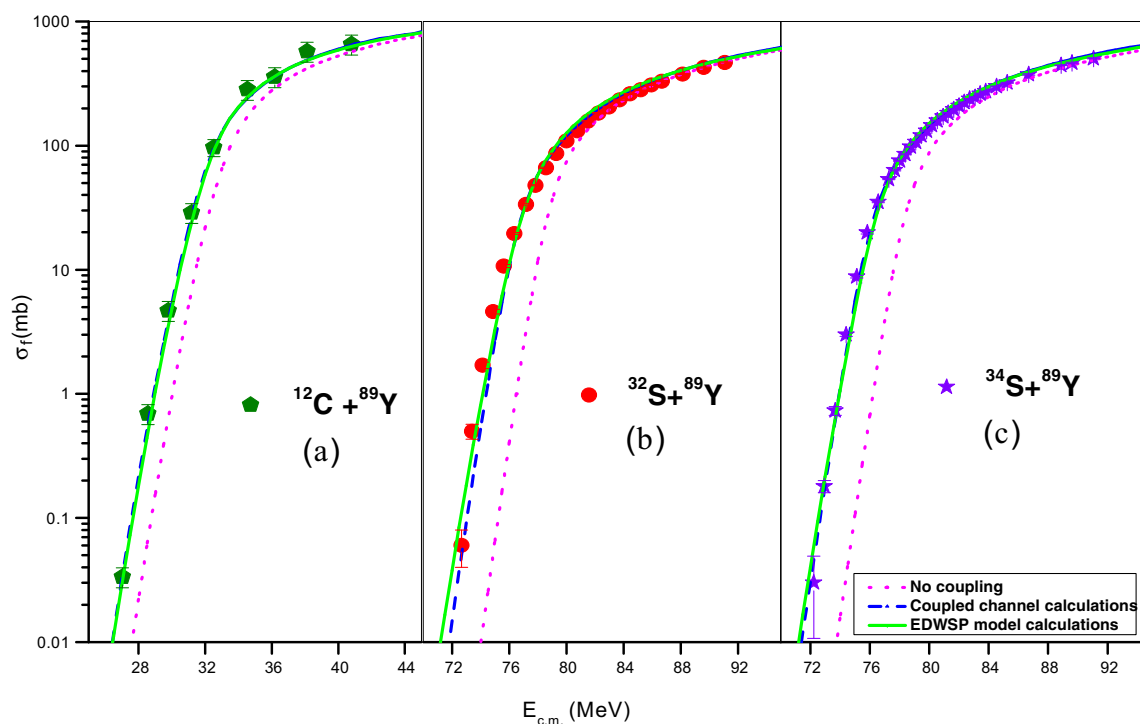


**Fig. 3** The fusion excitation functions of the  $^{12}\text{C} + ^{89}\text{Y}$  and  $^{32,34}\text{S} + ^{89}\text{Y}$  reactions obtained using the EDWSP model and the coupled channel code CCFULL. The results are compared with the available experimental data taken from ref. [21, 22]

allows one and two proton stripping channel with effective positive  $Q$  value ( $Q = +2.635$  MeV for one proton stripping and  $Q = +3.900$  MeV for two proton stripping), while the  $^{16}\text{S} + ^{89}\text{Y}$  system offers only single proton stripping with positive ground state  $Q$  value ( $Q = +0.589$  MeV).

In both cases, the experimental data is substantially larger than the predictions of no coupling scheme while the coupling to inelastic surface vibrations of the colliding nuclei significantly enhances the sub-barrier fusion cross section with respect to no coupling calculations. For both reactions, if projectile is taken as an inert, the coupling to single phonon  $2^+$  vibrational state alone or  $3^-$  vibrational states alone of the target fails to reproduce the fusion enhancement at sub-barrier energies. This clearly suggests the additions of the more intrinsic channels in the coupled channel analysis of the  $^{32,34}\text{S} + ^{89}\text{Y}$  reactions. The couplings to single phonon  $2^+$  vibrational state in projectile and single phonon  $2^+$  and  $3^-$  vibrational states along with their mutual couplings in target quantitatively improve the results but still could not address the fusion data at below barrier energies. With the inclusion of two phonon vibration in target and one phonon vibration in projectile along with their mutual coupling, the coupled channel calculations reasonably account the observed sub-barrier fusion enhancement. As the nucleon transfer channels have negligible influence on the fusion dynamics of the  $^{32,34}\text{S} + ^{89}\text{Y}$  systems, therefore the observed sub-barrier fusion enhancement of these reactions is the consequence of the

collective surface vibrations only. The lighter projectile is more collective than heavier projectile due to larger coupling strengths associated with the low lying inelastic surface excitations and these couplings in the coupled channel calculations reasonably address the observed sub-barrier fusion enhancement of the chosen reactions. The coupled channel calculations predicted that the larger sub-barrier fusion cross section of the  $^{32}\text{S} + ^{89}\text{Y}$  system (Fig. 3b) with respect to the  $^{34}\text{S} + ^{89}\text{Y}$  system (Fig. 3c) can be ascribed to the different collectivity of the projectiles. In both cases, the collectivity dominates over the nucleon (multi-nucleon) transfer channels, and hence, these intrinsic channels are the major factor that can be ascribed for the larger sub-barrier fusion enhancement over the expectations of the one-dimensional barrier penetration model. The similar conclusions are also reflected from the EDWSP model calculations wherein the greater amount of the barrier modification effects are introduced in lighter projectile with reference to the heavier projectile. In the literature, it is a well-established fact that the effect of the couplings between the relative motion of the colliding nuclei and nuclear structure degrees of freedom of the colliding systems is to replace the single Coulomb barrier into a distribution of barriers of different height and weight. This barrier distribution is the image of the type of couplings involved in the fusion mechanism and hence can be manifested for the occurrence of the larger fusion enhancement at below barrier energies. In the same

analogy, the EDWSP model results in a spectrum of the barriers of varying height (see Fig. 1), and as a consequence of barrier lowering effect, the EDWSP model adequately explained the observed sub-barrier fusion dynamics of the chosen reactions.

#### 4 Conclusions

To summarize, the present work is carried out to investigate the role of the projectile degrees of freedom in the fusion process. For this purpose, the fusion of the different projectiles ( ${}^9_4\text{Be}$ ,  ${}^{12}_6\text{C}$ , and  ${}^{32,34}_{16}\text{S}$ ) with a common target isotope ( ${}^{89}_{39}\text{Y}$ ) has been analyzed within the context of the EDWSP model and the coupled channel approach. In the case of the  ${}^{12}_6\text{C} + {}^{89}_{39}\text{Y}$  and  ${}^{16}_8\text{O} + {}^{89}_{39}\text{Y}$  reactions, the above-barrier fusion data is not suppressed and hence the stability of the projectiles against breakup effects is confirmed. The sub-barrier fusion enhancement of these reactions is regulated by the nuclear structure degrees of freedom of the colliding pairs, like inelastic surface excitations, while the proton transfer channels display a negligible influence on the sub-barrier fusion dynamics of these reactions. The coupled channel model and the EDWSP model-based calculations completely describe the observed fusion dynamics of the  ${}^{12}_6\text{C} + {}^{89}_{39}\text{Y}$  and  ${}^{32,34}_{16}\text{S} + {}^{89}_{39}\text{Y}$  reactions in the whole energy range around the Coulomb barrier. On the other hand, in case of the  ${}^9_4\text{Be} + {}^{89}_{39}\text{Y}$  reaction, the sub-barrier fusion enhancement occurs due to the nuclear structure degrees of freedom of the colliding system, while the above-barrier fusion data is suppressed as a consequence of the projectile breakup effects. The sub-barrier fusion enhancement of the chosen reaction is completely explained by the EDWSP model calculations and the coupled channel calculations. However, as one moves to above-barrier energy regions, both theoretical approaches predict larger fusion cross sections in comparison with the observed fusion data. Interestingly, the large deviations between the coupled channel calculations and the above-barrier fusion data are reduced to 10 % in the EDWSP model calculations. Therefore, within the context of the EDWSP model, the above-barrier fusion data is inhibited by a factor of 10 %, which is much smaller than a value reported in the literature. This physical effect occurs due to breakup of the projectile in the entrance channel before reaching the fusion barrier, and a part of the projectile fragment is fused with the target leading to the suppression effects at above barrier energies.

**Acknowledgments** This work was supported by Dr. D. S. Kothari Post-Doctoral Fellowship Scheme sponsored by University Grants Commission (UGC), New Delhi, India.

#### References

1. A.B. Balantekin, N. Takigawa, *Rev. Mod. Phys.* **70**, 77 (1998)
2. L.F. Canto et al., *Phys. Rep.* **424**, 1 (2006)
3. C.H. Dasso et al., *Phys. Rev. C* **50**, R12 (1994)
4. A. Diaz Torres et al., *Phys. Rev. C* **68**, 044607 (2003)
5. V. Tripathi et al., *Phys. Rev. Lett.* **88**, 172701 (2002)
6. J.J. Kolata et al., *Phys. Rev. Lett.* **81**, 4580 (1998)
7. N. Keeley et al., *Phys. Rev. C* **65**, 014601 (2002)
8. K.E. Zyromski et al., *Phys. Rev. C* **55**, R562 (1997)
9. M. Trotta et al., *Phys. Rev. Lett.* **84**, 2342 (2000)
10. M.S. Hussein et al., *Phys. Rev. C* **51**, 846 (1995)
11. C. Beck et al., *Phys. Rev. C* **67**, 054602 (2003)
12. M. Dasgupta et al., *Phys. Rev. C* **70**, 024606 (2004)
13. P.R.S. Gomes et al., *Phys. Rev. C* **73**, 064606 (2006)
14. P.R.S. Gomes et al., *Nucl. Phys. A* **828**, 233 (2009)
15. P.R.S. Gomes et al., *Phys. Lett. B* **634**, 356 (2006)
16. P.K. Rath et al., *Phys. Rev. C* **79**, 051601 (2009)
17. P.K. Rath et al., *Nucl. Phys. A* **874**, 14 (2012)
18. P.K. Rath et al., *Phys. Rev. C* **88**, 044617 (2013)
19. K. Hagino et al., *Phys. Rev. C* **61**, 037602 (2000)
20. A. Diaz Torres et al., *Phys. Rev. C* **65**, 024602 (2002)
21. C.S. Palshetkar et al., *Phys. Rev. C* **82**, 044608 (2010)
22. A. Mukherjee et al., *Phys. Rev. C* **66**, 034607 (2002)
23. M. Singh, Sukhvinder, R. Kharab, *Nucl. Phys. A* **897**, 179 (2013)
24. M. Singh, Sukhvinder, R. Kharab, *Nucl. Phys. A* **897**, 198 (2013)
25. M. Singh, Sukhvinder, R. Kharab, *Nucl. Phys. Mod. Phys. Lett. A* **26**, 2129 (2011)
26. M.S. Gautam, *Phys. Rev. C* **90**, 024620 (2014)
27. M.S. Gautam et al., *Phys. Rev. C* **92**, 054605 (2015)
28. M.S. Gautam, *Nucl. Phys. A* **933**, 272 (2015)
29. M.S. Gautam, *Acta Phys. Pol. B* **46**, 1055 (2015)
30. M.S. Gautam, *Chinese Phys. C* **39**, 114102 (2015)
31. K. Hagino, N. Rowley, A.T. Kruppa, *Comput. Phys. Commun.* **123**, 143 (1999). **K. Hagino (private communication)**
32. D.L. Hill, J.A. Wheeler, *Phys. Rev.* **89**, 1102 (1953)
33. C.Y. Wong, *Phys. Rev. Lett.* **31**, 766 (1973)
34. C.R. Morton et al., *Phys. Rev. C* **60**, 044608 (1999)
35. J.O. Newton et al., *Phys. Rev. C* **70**, 024605 (2004)
36. A. Mukherjee et al., *Phys. Rev. C* **75**, 044608 (2007)
37. L.C. Chamon et al., *Phys. Rev. C* **66**, 014610 (2002)
38. K. Washiyama, D. Lacroix, *Phys. Rev. C* **74**, 024610 (2008)
39. C. Simenel, M. Dasgupta, D.J. Hinde, E. Williams, *Phys. Rev. C* **88**, 064604 (2013)
40. T. Rumin, K. Hagino, N. Takigawa, *Phys. Rev. C* **61**, 014605 (1999)
41. Z.F. Muhammad et al., *Phys. Rev. C* **77**, 014606 (2008)
42. E.F. Aguilera, J.J. Kolata, *Phys. Rev. C* **85**, 014603 (2012)
43. M.S. Gautam, *Can. J. Phys.* **93**, 1343 (2015)
44. M.S. Gautam, *Mod. Phys. Lett. A* **30**, 1550013 (2015)
45. M.S. Gautam, *Phys. Scr.* **90**, 025301 (2015)
46. M.S. Gautam, *Phys. Scr.* **90**, 055301 (2015)
47. M.S. Gautam, *Phys. Scr.* **90**, 125301 (2015)
48. A. Shrivastava et al., *Phys. Rev. C* **63**, 054602 (2001)
49. T. Kibedi, R.H. Spear, *At. Data Nucl. Data Tables* **80**, 35 (2002)
50. A.S. Umar, C. Simenel, V.E. Oberacker, *Phys. Rev. C* **89**, 034611 (2014)
51. R. Kesar, A.S. Umar, V.E. Oberacker, *Phys. Rev. C* **85**, 044606 (2012)